

UCSF

UC San Francisco Electronic Theses and Dissertations

Title

Differing Patterns of Brain Connectivity in Autism Spectrum Disorder vs Sensory Processing Disorder

Permalink

<https://escholarship.org/uc/item/28n466v6>

Author

Chang, YiShin

Publication Date

2013

Peer reviewed|Thesis/dissertation

Differing Patterns of Brain Connectivity in Autism Spectrum Disorder
vs Sensory Processing Disorder

by

Yi-Shin Chang

THESIS

Submitted in partial satisfaction of the requirements for the degree of

MASTER OF SCIENCE

in

Biomedical Imaging



in the

GRADUATE DIVISION

of the

UNIVERSITY OF CALIFORNIA, SAN FRANCISCO

Copyright 2013

by

YiShin Chang

Differing Patterns of Brain Connectivity in Autism Spectrum Disorder vs. Sensory Process Disorder

Shin Chang

Abstract

Sensory Processing Disorders (SPD) affect 5-16% of children in the US, and have been shown to impair intellectual and social development due to disrupted processing and integration of sensory input. SPD exists both comorbidly with other neuropathologies such as autism spectrum disorder (ASD) and attention deficit hyperactivity disorder (ADHD), but often also exists in isolation. In our previous work, tract-based spatial statistics (TBSS) were used with diffusion tensor imaging (DTI) data of SPD subjects to demonstrate decreased white matter integrity in parieto-occipital white matter tracts.

Autism Spectrum Disorders (ASD) are typically clinically characterized by impaired communication, social interaction, and behavioral flexibility. However, the majority of individuals with ASD also exhibit sensory processing differences. It is valuable to characterize the similarities and differences in sensory processing deficits between sensory processing deficits within SPD and ASD for differential diagnosis and potentially for treatment planning.

We validate and expand upon previous white matter studies of ASD and our previous results in SPD by taking a tractographical approach to examining white matter tracts that we expect to be commonly and differentially affected in SPD vs ASD. Diffusion tensor imaging data was acquired in 16 boys with SPD, 15 boys with ASD, and 23 typically developing boys. Probabilistic fiber tractography was

then used with this data to delineate white matter tracts of interest, and white matter structural integrity was assessed for each of these tracts using average values of fractional anisotropy, mean diffusivity, radial diffusivity, and axial diffusivity within each tract. Significant decreases in FA were found for both the SPD and ASD cohorts within the parieto-occipital tracts as compared with the control cohort, with the SPD cohort demonstrating surprisingly and pervasively more affected FAs. Significant decreases in FA were found for the ASD cohort, but not the SPD cohort, within the temporal white matter tracts.

These findings validate abnormal white matter as a biological basis for SPD, demonstrate differential white matter pathology between ASD and SPD, and suggest that tracts contributing to social and emotional processing (and implicated in ASD) are independent of sensory processing.

TABLE OF CONTENTS

ABSTRACT	iii
LIST OF FIGURES	vi
LIST OF TABLES	vii
INTRODUCTION	1
MATERIALS AND METHODS	4
RESULTS	12
DISCUSSION	21
CONCLUSION	25
REFERENCES	26

LIST OF FIGURES

Figure 1. Delineated white matter tracts	11
Figure 2. Average overlap between tracts	13
Figure 3. Group differences of FA in temporal tracts	16
Figure 4. Group differences of FA in parieto-occipital tracts	16
Figure 5. Group differences of FA in frontal tracts	17

LIST OF TABLES

Table 1. Tractographical approach for temporal tracts	10
Table 2. Tractographical approach for parieto-occipital tracts	10
Table 3. Tractographical approach for frontal tracts	10
Table 4. Group differences of FA	17
Table 5. Group differences of MD	18
Table 6. Group differences of RD	18
Table 7. Group differences of AD	19

1. Introduction

5-16% of children in the US are affected by primary sensory processing disorders (SPD), which have been shown to impair intellectual and social development as a result of disrupted processing and integration of information from multiple sensory modalities (Ahn et al., 2004, Ben-Sasson et al., 2009a, Brett-Green et al., 2008, and Bundy et al., 2007). SPD exists comorbidly with pathologies such as autism spectrum disorder (ASD) and attention deficit hyperactivity disorder (ADHD), but also frequently exists independently of these other psychopathologies. Despite its prevalence, SPD has been sparingly investigated. Studies are therefore needed to understand the neural substrates underlying SPD, with particular attention to the differentiation of its isolated form from its expression in more well-investigated psychopathologies such as ASD. A better understanding of the similarities and differences in sensory processing deficits between these psychopathologies will be crucial for differential diagnosis and treatment planning (Baranek et al., 2007).

We have previously demonstrated that children with SPD are affected by decreased microstructural integrity primarily in posterior white matter, which contributes to primary sensory processing, and that this integrity correlates strongly with behavioral measures of sensory processing function and multisensory integration (Owen et al., 2013). Microstructural characteristics of white matter tracts are crucial in the determination of the speed and bandwidth of information transmission through the brain. Abnormalities of this microstructure

in the primary sensory tracts or in tracts connecting multimodal association areas can thereby result in the loss of precise timing of action potential propagation and impairment of accurate sensory processing and integration (Basser et al., 1994, Mori et al., 1999 and Mukherjee et al., 2008).

The advent of diffusion tensor imaging (DTI) has enabled noninvasive evaluation of white matter connectivity and integrity through quantitative parameters that measure different properties of water diffusivity and reflect microstructural properties such as axon diameter, degree of myelination, fiber packing density, and fiber collimation (Beaulieu, 2002 and Mukherjee et al., 2008). The most widely used of these parameters is fractional anisotropy (FA), which represents the degree to which water diffusivity depends on orientation. Additionally, mean diffusivity (MD) is the rate of diffusion averaged over all directions, axial diffusivity (AD) is the rate of diffusion along the orientation of white matter fibers within a tract, and radial diffusivity (RD) is the rate of diffusion orthogonal to fiber orientation. In conjunction, these parameters provide a valuable quantitative characterization of white matter organization, with alterations in parameter values reflecting white matter pathology. Generally, white matter pathology will result in decreased FA, elevated MD, and elevated RD (Mukherjee et al., 2008).

Autism spectrum disorders (ASD) are clinically characterized by impaired communication, social interaction, and behavioral flexibility (American Psychiatric Association, 1994). Both molecular and functional connectivity

studies of ASD have suggested decreased connectivity between frontal and posterior areas of the brain as the neural basis of uneven cognitive profiles in individuals with ASD (Travers et al., 2012). DTI studies of ASD have demonstrated decreases in FA in white matter tracts spanning across many regions of the brain, with consistent decreases in the corpus callosum (CC), the cingulum, and tracts connecting aspects of the temporal lobe (Travers et al., 2012). There is a need, however, to understand how these neural markers are related to specific patterns of behavior and cognition in those affected by ASD. While the ASD phenotype arises from many different known etiologies, and with high variability of cognitive ability, the majority of individuals with ASD report sensory processing differences (Marco et al., 2011). This is therefore a valuable cohort to study in comparison to an SPD cohort in which sensory processing differences exist in isolation.

In addition to the quantitative characterization of white matter, DTI has enabled the anatomic mapping of white matter tracts through fiber tractography. By utilizing orientation-dependent variations in diffusion-weighted signal intensity, DTI allows for a 3D tensor to be fit to the angular variation in rate of diffusion at every voxel. DTI fiber tracking then uses the diffusion tensor at each voxel to follow axonal tracts from voxel to voxel, ultimately delineating entire white matter tracts in the human brain (Mukherjee et al., 2008).

In this study, we take a tractography-based, hypothesis-driven approach to examining white matter in tracts that we hypothesize to be commonly and differentially affected in SPD and ASD subjects compared to typically developing children (TDC). By using tractography, we are able to assess whole-tract white matter integrity in the native space of each subject. Based upon our previous work with SPD (Owen et al., 2013), and upon previous studies of white matter in ASD (Travers et al., 2012), we hypothesize that SPD subjects will be primarily affected in parieto-occipital white matter tracts involved with primary sensory processing, while ASD subjects will be affected in temporal tracts associated with social and emotional processing in addition to parieto-occipital tracts.

2. Methods

2.1. Demographic, sensory, cognitive and behavioral data

2.1.1. General demographics and sensory, cognitive and behavioral assessment

Sixteen right-handed males with SPD, fifteen males with ASD (12 right-handed, 1 left-handed, 2 ambidextrous), and 23 right-handed male TDCs, all between 8 and 11 years of age, were prospectively enrolled under our institutional review board approved protocol. Subjects were recruited from the Autism & Neurodevelopment Program and from local online parent board listings. Informed consent was obtained from the parents or legal guardians, with the assent of all participants.

All subjects were assessed with the Wechsler Intelligence Scale for Children-Fourth Edition (Wechsler, 2003), the Sensory Profile (Dunn and Westman, 1997), and the social communication questionnaire (SCQ). The Sensory Profile is a

parent report questionnaire which measures behavioral sensory differences, yielding scores within individual sensory domains and factors and a total score. The Sensory Profile score is used in addition to a behavioral assessment for diagnosis of SPD. The social communication questionnaire (SCQ) is a parent report screening test used to diagnose ASD (Eaves et al., 2006).

All but one of the SPD subjects scored in the definite difference range of the total Sensory Profile, with the remaining subject scoring in the probable difference range. Nine of the ASD subjects scored in the definite difference range of the total Sensory Profile, two of the ASD subjects scored in the probable difference range, three scored in the normal range, and one was not administered the Sensory Profile. All of the controls scored in the normal range.

2.1.2. Autism Spectrum Disorder

Three of the boys with SPD, but none of the typically developing children, had abnormally high scores on the social communication questionnaire (SCQ), a parent report screening test for ASD (Eaves et al., 2006). The parents of these three subjects were further administered the full Autism Diagnostic Inventory-Revised (ADIR) (Lord et al., 1994) and the three children themselves were tested with the Autism Diagnostic Observation Schedule (ADOS) (Lord et al., 1989). One of the boys scored in the range of ASD on the ADOS and another was found to be in the ASD range on the ADIR, but none met the criteria for ASD on both exams. Evaluation of these three subjects by Dr. Marco, a child neurologist experienced in autism, was also not consistent with an ASD diagnosis.

All but one of the ASD subjects scored in the ASD range of the SCQ, all but one of the ASD subjects scored in the ASD range of the ADIR (a different subject than the SCQ-normal subject), and all ASD subjects scored in the abnormal ranges of the ADOS.

2.1.3. Attention deficits

On the inattention measure of the Sensory Profile, eleven of the 16 SPD subjects scored in the definite difference range, four in the probable difference range, and one in the typical range. Of the 15 ASD subjects, seven scored in the definite difference range, three scored in the probable difference range, three scored in the typical difference range, and one was not administered the Sensory Profile. Of the 23 typically developing children, none scored in the definite difference range, three in the probable difference range, and twenty in the typical range. Abnormal inattention scores on the Sensory Profile do not qualify subjects for an ADHD diagnosis.

2.1.4. Prematurity

Three of 16 SPD boys were born prematurely, one at 32 weeks gestation and two at 34 weeks gestation. One of the 24 typically developing children was born prematurely, at 33 weeks gestation. These four subjects were found to be in the middle of the distribution for global FA and mean FA extracted from clusters of significantly affected voxels using tract-based spatial statistics for their respective groups, and therefore did not represent outliers. None of the ASD subjects were born prematurely.

2.2. Image acquisition

MR imaging was performed on a 3T Tim Trio scanner (Siemens, Erlangen, Germany) using a 12-channel head coil. Structural MR imaging of the brain was performed with an axial 3D magnetization prepared rapid acquisition gradient-echo T1-weighted sequence (TE = 2.98 ms, TR = 2300 ms, TI = 900 ms, flip angle of 9°) with a 256 mm field of view (FOV), and 160 1.0 mm contiguous partitions at a 256 × 256 matrix. Whole-brain DTI was performed with a multislice 2D single-shot twice-refocused spin-echo echo-planar sequence with 64 diffusion-encoding directions, diffusion-weighting strength of $b = 2000 \text{ s/mm}^2$, iPAT reduction factor of 2, TE/TR = 109/8000 ms, averages = 1, interleaved 2.2 mm axial slices with no gap, and in-plane resolution of 2.2 × 2.2 mm with a 100 × 100 matrix and FOV of 220 mm. An additional image volume was acquired with no diffusion weighting ($b = 0 \text{ s/mm}^2$). The total DTI acquisition time was 8.67 min.

2.3. DTI analysis

2.3.1. Pre-processing

The diffusion-weighted images were corrected for motion and eddy currents using FMRIB's Linear Image Registration Tool (FLIRT; www.fmrib.ox.ac.uk/fsl/flirt) with 12-parameter linear image registration (Jenkinson et al., 2002). All diffusion-weighted volumes were registered to the reference $b = 0 \text{ s/mm}^2$ volume. To evaluate subject movement, we calculated a scalar parameter quantifying the transformation of each diffusion volume to the reference. A heteroscedastic two-sample Student's t-test verified that there were no significant differences between

SPD, ASD, and TDC groups in movement during the DTI scan ($p > 0.05$). The non-brain tissue was removed using the Brain Extraction Tool (BET; <http://www.fmrib.ox.ac.uk/analysis/research/bet>). FA, MD, AD and RD were calculated using FSL's DTIFIT.

2.3.2. HARDI reconstruction and fiber tractography

FMRIB's BEDPOSTX tool was used for HARDI reconstruction of the diffusion data, modeling multiple fiber orientations per voxel, and thereby allowing for sensitivity to crossing fibers. Probabilistic tractography was performed using probtrackx2 to delineate white matter tracts of interest. Seed, waypoint, termination, and exclusion masks for tractography were primarily derived from the gray-white matter boundaries (GWB) of the 82 FreeSurfer cortical and subcortical regions, which were automatically segmented on the T1-weighted MR images using FreeSurfer 5.1.0 (Fischl, 2012) and registered using a linear affine transformation to diffusion space using FLIRT. The left and right cerebral peduncles were manually defined for each subject.

2.3.3 Tract delineation

After tractography was run, tract masks were created by thresholding the resultant connectivity distribution at 1 percent of the maximum number of streamlines that passed through any given voxel. In other words, a given voxel was retained in the mask if the number of streamlines passing through it exceeded one percent of the maximum number of streamlines in the connectivity distribution. The resultant masks were then thresholded using FA maps, only retaining voxels for which FA

was greater than 0.2. The masks for each white matter tract were used to determine average FA, MD, RD, and AD values within each tract for each subject.

The tractographical approaches to delineating each of the tracts presented in this paper are summarized in Tables 1, 2, and 3, and representative tracts are displayed in Figure 1. All masks used for tractography were the GWBs of Freesurfer regions except for manually-defined cerebral peduncles and corpus callosum masks.

Eroded thalamus masks refer to an eroded version of the Freesurfer thalamus which was transformed using the *fslmaths* erode filtering operation with a box kernel of width 9, a step taken to prevent the thalamic mask from overlapping the corpus callosum and resulting in spurious interhemispheric streamlines. Excepting callosal connections, each tract was delineated separately in both the left and right hemispheres. Following mask extraction (after thresholding by streamlines and FA), corresponding left and right hemisphere tract masks were combined for subsequent analysis. The unilateral tracts were also individually assessed to confirm bilateral consistency, and to evaluate hypothesized tract laterality.

Table 1. Tractographical approach for temporal tracts. *Orbitofrontal cortex was created by summing the medial orbitofrontal cortex and lateral orbitofrontal cortex.

White matter tract	Seed mask	Waypoint and termination mask	Exclusion mask
Fusiform - amygdala	Fusiform gyrus	Amygdala	All other gm regions
Fusiform - hippocampus	Fusiform gyrus	Hippocampus	All other gm regions
Uncinate fasciculus	Orbitofrontal cortex*	Entorhinal cortex + temporal pole	All other gm regions
Inferior longitudinal fasciculus (ILF)	Pericalcarine cortex	Inferior temporal cortex	Thalamus + all other cortical regions
Inferior frontooccipital fasciculus (IFOF)	Lingual gyrus	Orbitofrontal cortex*	Thalamus + all other cortical regions

Table 2. Tractographical approach for parieto-occipital tracts. *For the tract through the splenium of the corpus callosum, a callosal waypoint mask was also used.

White matter tract	Seed mask	Waypoint and termination mask	Exclusion mask
Optic radiation	Pericalcarine cortex	Eroded thalamus	All other cortical regions
Dorsal visual stream	Pericalcarine cortex	Inferior parietal cortex	Thalamus
Splenium of the corpus callosum	Left lateral occipital cortex	Right lateral occipital cortex*	All other cortical regions
Posterior corona radiata (PCR) (occipital)	All occipital regions	Cerebral peduncle	All other cortical regions
Posterior corona radiata (PCR) (parietal)	All parietal regions	Cerebral peduncle	All other cortical regions

Table 3. Tractographical approach for parieto-occipital tracts. *For the tracts through the genu of the corpus callosum, a callosal waypoint mask was also used.

White matter tract	Seed mask	Waypoint and termination mask	Exclusion mask
Anterior thalamic radiation (ATR) (medial orbitofrontal cortex)	Medial orbitofrontal cortex	Eroded thalamus	All other gm regions
Anterior thalamic radiation (ATR) (rostral middle frontal cortex)	Rostral middle frontal cortex	Eroded thalamus	All other gm regions
Genu of the corpus callosum (medial orbitofrontal cortex)	Left medial orbitofrontal cortex	Right medial orbitofrontal cortex	All other cortical regions
Genu of the corpus callosum (rostral middle frontal cortex)	Left rostral middle frontal cortex	Right rostral middle frontal cortex	All other cortical regions
Anterior corona radiata (ACR)	All frontal regions	Cerebral peduncle	All other cortical regions

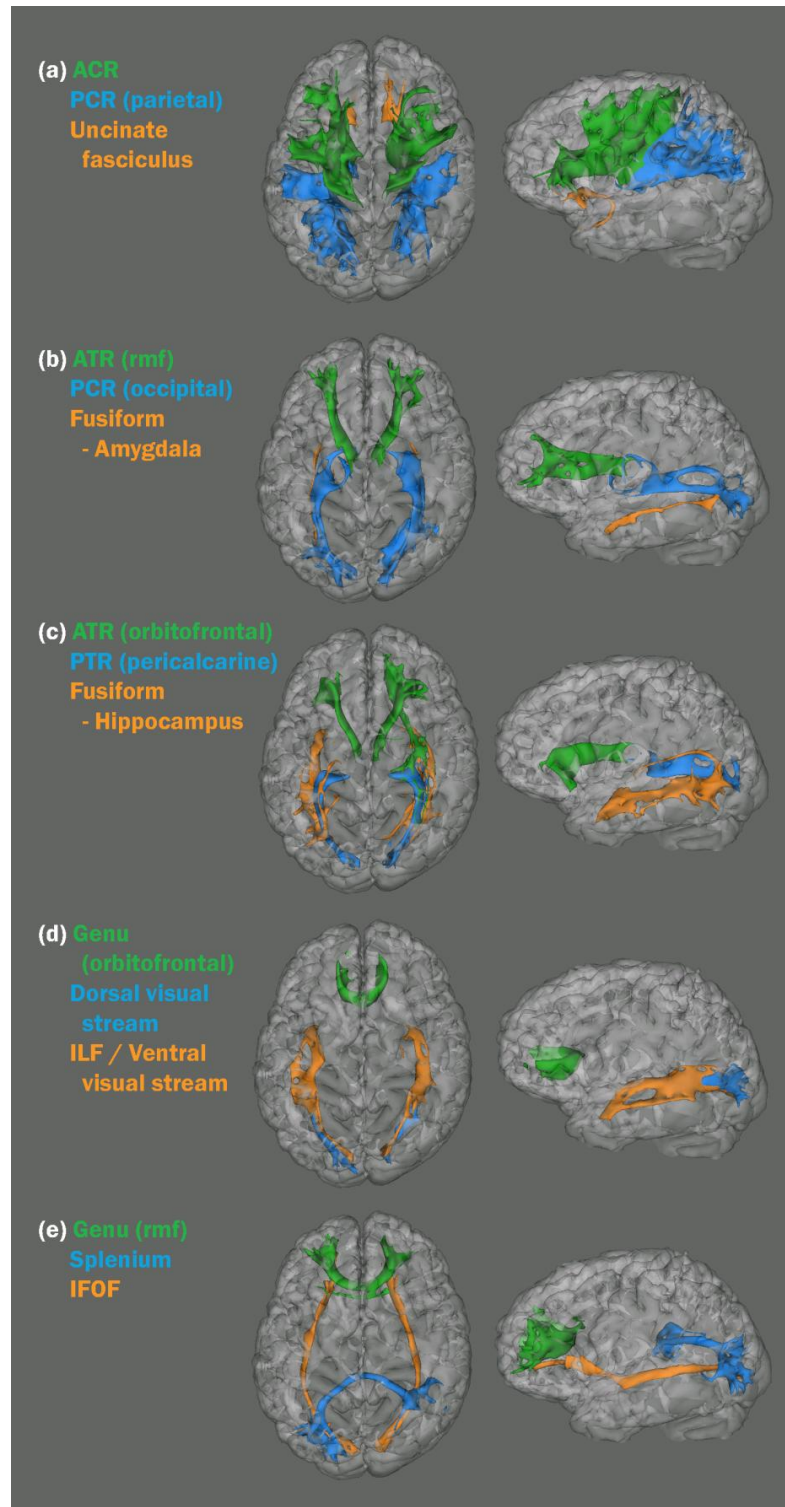


Figure 1. Examples of each delineated tract for a representative subject. Green masks represent frontal tracts, blue masks represent parietal-occipital tracts, and orange masks represent temporal tracts. The tracts are superimposed upon the T1 image, registered to diffusion space and with decreased opacity, of the representative subject.

2.4. Statistical Analysis

For each tract, two-tailed nonparametric permutation tests (n=10,000) were performed using a two-sample t-statistic (adapted from *Nichols et al., 2001*) between the mean FA, MD, RD, and AD values of SPD subjects and TDC subjects, as well as between ASD subjects and TDC subjects. Group differences were assessed at a significance level of $p < 0.05$.

3. Results

3.1. Tract overlap

Some tracts demonstrated a significant fraction of shared voxels. Figure 2 depicts the average fraction of each tract's voxels that are shared with every other investigated white matter tract. In the most severe case, a subject average of 77% of the fusiform - amygdala tract voxels are contained within the fusiform - hippocampus tract. There are also significant overlaps within the delineated parietal-occipital tracts, and between some parietal-occipital and temporal tracts. These results are presented here for disclosure in interpreting independence of the following group difference results.

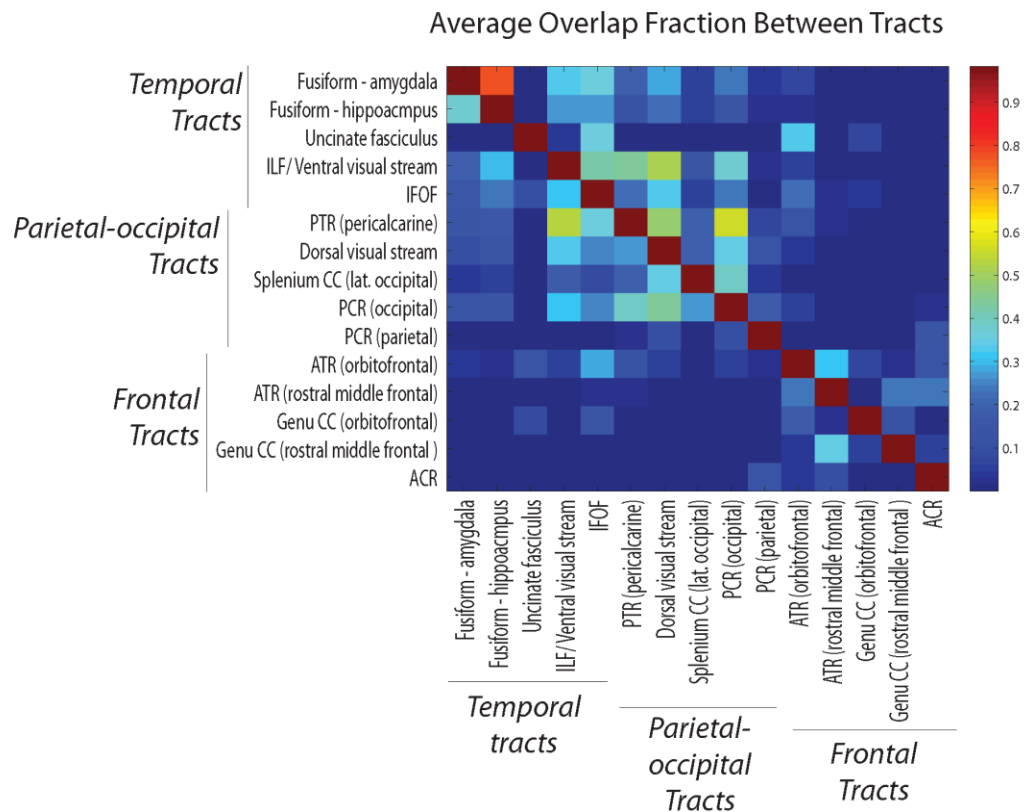


Figure 2. Average fraction of tract overlap, where the color intensity corresponds to the subject average of the fraction of the voxels of the tracts on the vertical axis that are contained within the tracts on the horizontal axis.

3.2. Group Differences in FA

Figures 2-4 depict group differences in FA in temporal, parietal-occipital, and frontal tracts. Table 1 details group differences in FA in each tract.

3.2.1. Group differences of FA in Temporal tracts

Significantly lower values of FA were detected between the TDC and the ASD boys in the fusiform to amygdala and fusiform to hippocampus tracts ($p < 0.01$), while no significant differences were detected between the TDC and the SPD

boys in these tracts. There was no significant difference between the FA values of the uncinate fasciculi of any of the cohorts.

Significantly lower FA values were detected for the ASD boys compared to TDC in the inferior longitudinal fasciculi and the inferior fronto-occipital fasciculi ($p < 0.05$), while lower FA values were detected for the SPD boys compared to TDC in the inferior longitudinal fasciculi, but not the inferior fronto-occipital fasciculi. In all of the temporal white matter tracts, the FA values were more affected in the ASD subjects than in the SPD subjects.

3.2.2. Group differences of FA in Parietal-Occipital Tracts

Significantly lower values of FA were detected for the SPD boys compared to the TDC boys in the dorsal visual stream ($p < 0.01$), the callosal visual tract through the splenium of the corpus callosum ($p < 0.05$), and the posterior corona radiata to the occipital lobe ($p < 0.05$). The FA values in the posterior thalamic radiation to the visual cortex and the posterior corona radiata to the parietal lobe trended lower for the SPD boys, but were not statistically significantly different.

Significantly lower FA values were detected for the ASD boys compared to the TDC boys in the dorsal visual stream and the PCR to the occipital lobe, but not in other posterior tracts. For the posterior tracts in which the ASD cohort was affected, the difference in FA was intermediate compared to the differences exhibited in the SPD cohort.

3.2.3. Group differences of FA in Frontal Tracts

Significantly lower values of FA were detected for the SPD boys compared to the TDC boys in the anterior thalamic radiation ($p < 0.05$). The FA values in the other frontal tracts were not significantly different between the TDC and the SPD boys, though the SPD FA values trended lower in each case.

Significantly higher values of FA were detected for the ASD boys compared to the TDC boys in the anterior corona radiata ($p < 0.05$). The FA values in the other frontal tracts were not significantly different between the TDC and the ASD boys.

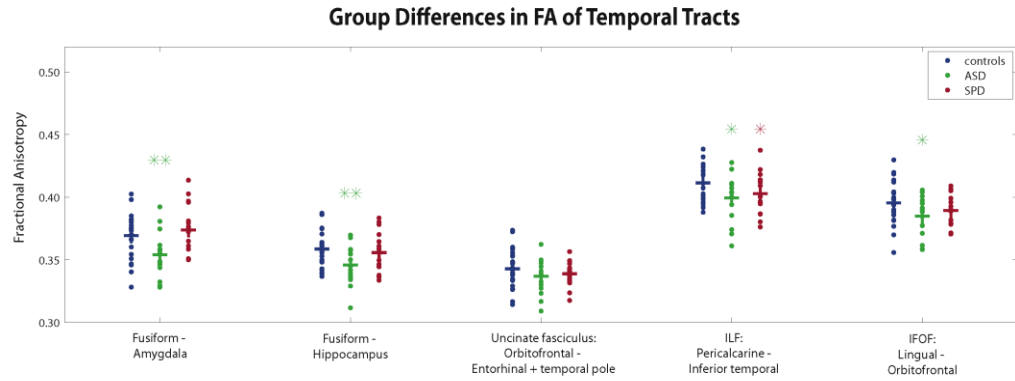


Figure 3. Group differences between TDC, SPD, and ASD subjects in average FA within different temporal tracts. Green asterisks depict group differences between ASD and TDC subjects, and red asterisks depict group differences between SPD and TDC subjects, where one asterisk indicates a significance level of $p < 0.05$ and two asterisks indicate a significance level of $p < 0.01$.

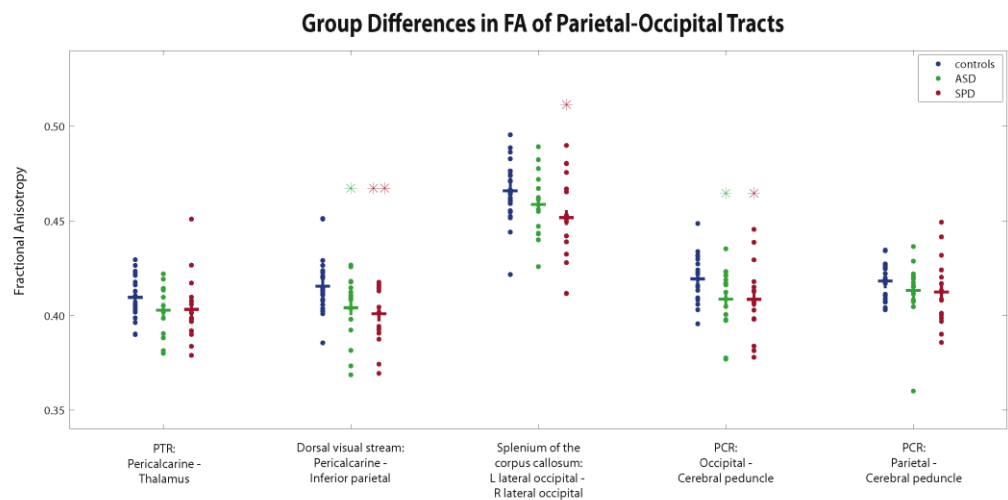


Figure 4. Group differences between TDC, SPD, and ASD subjects in average FA within different parietal-occipital tracts. Green asterisks depict group differences between ASD and TDC subjects, and red asterisks depict group differences between SPD and TDC subjects, where one asterisk indicates a significance level of $p < 0.05$ and two asterisks indicate a significance level of $p < 0.01$.

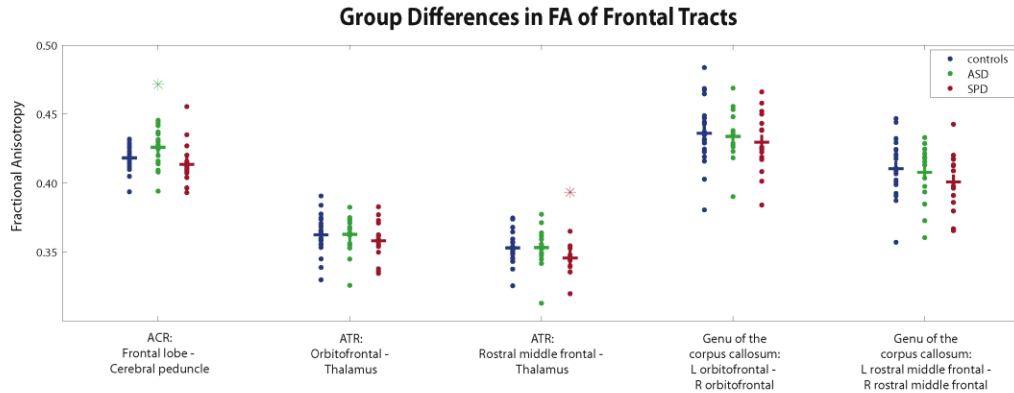


Figure 5. Group differences between TDC, SPD, and ASD subjects in average FA within different frontal tracts. Green asterisks depict group differences between ASD and TDC subjects, and red asterisks depict group differences between SPD and TDC subjects, where one asterisk indicates a significance level of $p < 0.05$ and two asterisks indicate a significance level of $p < 0.01$.

Table 4. Group differences of fractional anisotropy (FA) in all tracts. Red highlighted cells depict significant group differences between SPD and TDC subjects, green highlighted cells depict significant group differences between ASD and TDC subjects. *Excepting the ACR, all tracts showing significant group differences demonstrate higher FA for the control cohorts.

Tract	TDC		SPD		P-val	ASD		P-val
	mean FA	SD	mean FA	SD		mean FA	SD	
Fusiform - amygdala	0.3693 ±	0.0182	0.3738 ±	0.0203	0.2373	0.3546 ±	0.0177	0.0089
Fusiform - hippocampus	0.3587 ±	0.0146	0.3558 ±	0.0160	0.2749	0.3469 ±	0.0156	0.0099
Uncinate fasciculus	0.3429 ±	0.0156	0.3388 ±	0.0099	0.1878	0.3375 ±	0.0137	0.1375
ILF	0.4114 ±	0.0147	0.4028 ±	0.0164	0.0456	0.4008 ±	0.0192	0.0290
IFOF	0.3956 ±	0.0171	0.3893 ±	0.0128	0.1154	0.3844 ±	0.0156	0.0220
PTR	0.4095 ±	0.0113	0.4032 ±	0.0175	0.0871	0.4029 ±	0.0127	0.0512
Dorsal visual stream	0.4155 ±	0.0147	0.4009 ±	0.0156	0.0025	0.4052 ±	0.0179	0.0277
Splenium of the CC (lat occipital)	0.4658 ±	0.0161	0.4517 ±	0.0238	0.0176	0.4589 ±	0.0167	0.0993
PCR (occipital)	0.4194 ±	0.0123	0.4085 ±	0.0190	0.0168	0.4093 ±	0.0161	0.0167
PCR (parietal)	0.4182 ±	0.0093	0.4124 ±	0.0178	0.1037	0.4142 ±	0.0168	0.1957
ACR	0.4182 ±	0.0091	0.4136 ±	0.0156	0.1253	0.4259 ±	0.0146	0.0240*
ATR (orbitofrontal)	0.3623 ±	0.0137	0.3581 ±	0.0140	0.1748	0.3627 ±	0.0137	0.4704
ATR (rostral middle frontal)	0.3530 ±	0.0111	0.3457 ±	0.0105	0.0234	0.3532 ±	0.0143	0.4671
Genu of the CC (orbitofrontal)	0.4361 ±	0.0224	0.4296 ±	0.0218	0.1828	0.4338 ±	0.0179	0.3676
Genu of the CC (rostral middle frontal)	0.4105 ±	0.0196	0.4008 ±	0.0204	0.0753	0.4078 ±	0.0208	0.3448

Table 5. Group differences of mean diffusivity (MD) in all tracts. Red highlighted cells depict significant group differences between SPD and TDC subjects, green highlighted cells depict significant group differences between ASD and TDC.

Tract	TDC mean MD (10E-3) ± SD (10E-3)	SPD mean MD (10E-3) ± SD (10E-3)	P-val	ASD mean MD (10E-3) ± SD (10E-3)	P-val
Fusiform - amygdala	0.6768 ± 0.0214	0.6931 ± 0.0248	0.0182	0.0374 ± 0.0217	0.0760
Fusiform - hippocampus	0.6768 ± 0.0201	0.6938 ± 0.0251	0.0132	0.0364 ± 0.0238	0.0699
Uncinate fasciculus	0.6932 ± 0.0306	0.6963 ± 0.0300	0.3726	0.4759 ± 0.0202	0.9528
ILF	0.6867 ± 0.0171	0.7054 ± 0.0289	0.0083	0.0420 ± 0.0174	0.0778
IFOF	0.6861 ± 0.0180	0.7022 ± 0.0225	0.0083	0.1271 ± 0.0197	0.2382
PTR	0.6814 ± 0.0147	0.6982 ± 0.0228	0.0051	0.0693 ± 0.0177	0.1333
Dorsal visual stream	0.6739 ± 0.0160	0.6910 ± 0.0259	0.0078	0.0744 ± 0.0213	0.1407
Splenium of the CC (lat occipital)	0.6836 ± 0.0201	0.7036 ± 0.0282	0.0073	0.3399 ± 0.0236	0.6740
PCR (occipital)	0.6670 ± 0.0179	0.6860 ± 0.0248	0.0044	0.0766 ± 0.0190	0.1535
PCR (parietal)	0.6593 ± 0.0185	0.6738 ± 0.0183	0.0110	0.1898 ± 0.0240	0.3688
ACR	0.6464 ± 0.0173	0.6569 ± 0.0177	0.0362	0.3765 ± 0.0172	0.7435
ATR (orbitofrontal)	0.6678 ± 0.0223	0.6706 ± 0.0238	0.3574	0.4619 ± 0.0192	0.9187
ATR (rostral middle frontal)	0.6710 ± 0.0223	0.6845 ± 0.0233	0.0399	0.3136 ± 0.0135	0.6268
Genu of the CC (orbitofrontal)	0.6508 ± 0.0303	0.6572 ± 0.0293	0.2644	0.5080 ± 0.0239	0.9945
Genu of the CC (rostral middle frontal)	0.6721 ± 0.0298	0.6940 ± 0.0322	0.0158	0.1139 ± 0.0193	0.2365

Table 6. Group differences of radial diffusivity (RD) in all tracts. Red highlighted cells depict significant group differences between SPD and TDC subjects, green highlighted cells depict significant group differences between ASD and TDC.

Tract	TDC mean RD (10E-3) ± SD (10E-3)	SPD mean RD (10E-3) ± SD (10E-3)	P-val	ASD mean RD (10E-3) ± SD (10E-3)	P-val
Fusiform - amygdala	0.5363 ± 0.0233	0.5468 ± 0.0232	0.0881	0.5530 ± 0.0201	0.0136
Fusiform - hippocampus	0.5409 ± 0.0213	0.5550 ± 0.0225	0.0272	0.5563 ± 0.0226	0.0182
Uncinate fasciculus	0.5611 ± 0.0289	0.5659 ± 0.0264	0.3063	0.5629 ± 0.0186	0.4145
ILF	0.5243 ± 0.0184	0.5428 ± 0.0270	0.0073	0.5363 ± 0.0201	0.0311
IFOF	0.5310 ± 0.0211	0.5461 ± 0.0211	0.0174	0.5416 ± 0.0190	0.0585
PTR	0.5195 ± 0.0148	0.5350 ± 0.0236	0.0085	0.5287 ± 0.0151	0.0360
Dorsal visual stream	0.5120 ± 0.0179	0.5322 ± 0.0234	0.0015	0.5235 ± 0.0226	0.0442
Splenium of the CC (lat occipital)	0.4923 ± 0.0171	0.5149 ± 0.0283	0.0019	0.4981 ± 0.0234	0.1773
PCR (occipital)	0.5041 ± 0.0181	0.5237 ± 0.0253	0.0044	0.5155 ± 0.0183	0.0311
PCR (parietal)	0.4993 ± 0.0170	0.5132 ± 0.0207	0.0151	0.5063 ± 0.0253	0.1687
ACR	0.4900 ± 0.0154	0.5004 ± 0.0198	0.0344	0.4846 ± 0.0173	0.1522
ATR (orbitofrontal)	0.5340 ± 0.0218	0.5380 ± 0.0232	0.2929	0.5332 ± 0.0196	0.4567
ATR (rostral middle frontal)	0.5407 ± 0.0211	0.5549 ± 0.0210	0.0204	0.5428 ± 0.0164	0.3708
Genu of the CC (orbitofrontal)	0.4863 ± 0.0292	0.4931 ± 0.0290	0.2380	0.4877 ± 0.0229	0.4349
Genu of the CC (rostral middle frontal)	0.5136 ± 0.0289	0.5350 ± 0.0293	0.0147	0.5219 ± 0.0223	0.1692

Table 7. Group differences of axial diffusivity (AD) in all tracts. Red highlighted cells depict significant group differences between SPD and TDC subjects, green highlighted cells depict significant group differences between ASD and TDC subjects.

Tract	TDC mean AD (10E-3) ± SD (10E-3)	SD (10E-3)	SPD mean AD (10E-3) ± SD (10E-3)	SD (10E-3)	P-val	ASD mean AD (10E-3) ± SD (10E-3)	SD (10E-3)	P-val
Fusiform - amygdala	0.9579 ±	0.0231	0.9857 ±	0.0373	0.0035	0.9628 ±	0.0325	0.2931
Fusiform - hippocampus	0.9487 ±	0.0216	0.9715 ±	0.0359	0.0091	0.9575 ±	0.0315	0.1503
Uncinate fasciculus	0.9573 ±	0.0375	0.9572 ±	0.0390	0.4900	0.9522 ±	0.0277	0.3173
ILF	1.0115 ±	0.0194	1.0306 ±	0.0362	0.0203	1.0181 ±	0.0233	0.1779
IFOF	0.9963 ±	0.0196	1.0144 ±	0.0281	0.0110	0.9969 ±	0.0286	0.4669
PTR	1.0053 ±	0.0194	1.0247 ±	0.0271	0.0065	1.0108 ±	0.0290	0.2428
Dorsal visual stream	0.9978 ±	0.0177	1.0087 ±	0.0362	0.1140	1.0017 ±	0.0265	0.2960
Splenium of the CC (lat occipital)	1.0663 ±	0.0360	1.0810 ±	0.0410	0.1266	1.0636 ±	0.0323	0.4052
PCR (occipital)	0.9928 ±	0.0217	1.0104 ±	0.0301	0.0214	0.9960 ±	0.0283	0.3400
PCR (parietal)	0.9791 ±	0.0244	0.995 ±	0.0218	0.0233	0.9838 ±	0.0257	0.2776
ACR	0.9590 ±	0.0235	0.9697 ±	0.0182	0.0690	0.9644 ±	0.0228	0.2428
ATR (orbitofrontal)	0.9354 ±	0.0257	0.9359 ±	0.0281	0.4659	0.9348 ±	0.0222	0.4630
ATR (rostral middle frontal)	0.9316 ±	0.0263	0.9435 ±	0.0299	0.0942	0.9366 ±	0.0117	0.2393
Genu of the CC (orbitofrontal)	0.9798 ±	0.0410	0.9853 ±	0.0377	0.3335	0.9768 ±	0.0307	0.4038
Genu of the CC (rostral middle frontal)	0.9892 ±	0.0356	1.0119 ±	0.0453	0.0455	1.0031 ±	0.0235	0.0965

3.3. Group differences in MD, RD, and AD

Tables 2-4 depict group differences in MD, RD, and AD in each tract.

3.3.1. Group differences of MD, RD, and AD in Temporal Tracts

Significantly elevated values of MD, RD, and AD were detected for the SPD boys compared to the TDC boys in the fusiform to hippocampus tract, the ILF, and the IFOF ($p < 0.05$). The MD and AD values within the fusiform to amygdala tracts were also significantly elevated for the SPD boys compared to the TDC boys ($p < 0.05$).

Significantly elevated values of MD and RD were detected for the ASD boys compared to the TDC boys in the ILF ($p < 0.05$). Significantly elevated values of RD were also detected for the ASD boys compared to the TDC boys in the fusiform to amygdala and fusiform to hippocampus tracts ($p < 0.05$).

3.3.2. Group differences of MD, RD, and AD in Parietal-Occipital Tracts

Significantly elevated values of MD and RD were detected for the SPD boys compared to the TDC boys in the posterior thalamic radiation, the dorsal visual stream, the callosal visual tract through the splenium of the corpus callosum, and the posterior corona radiata to both the occipital and parietal lobes ($p < 0.01$ except for RD in PCR to the parietal lobe ($p < 0.05$)). AD was also significantly elevated for the SPD boys in the PTR and PCR to both the occipital and parietal lobes.

The MD and RD values of the ASD boys trended higher than those of the TDC boys in all of the parietal-occipital tracts, appearing to be intermediately affected compared to the SPD boys. The RD values were statistically significantly elevated in the PTR, dorsal visual stream, and PCR to the occipital lobe ($p < 0.05$). There were no statistically significant differences between the AD values of the ASD boys in these tracts compared to the TDC boys.

3.3.3. Group differences of MD, RD, and AD in Frontal Tracts

Significantly elevated values of MD and RD were detected for the SPD boys compared to the TDC boys in the ACR, the ATR from the rostral middle frontal cortex, and the homotopic tract between the rostral middle frontal cortices through the genu of the corpus callosum. The AD value was also significantly elevated for the SPD subjects in the homotopic tract between the rostral middle frontal cortices through the genu of the corpus callosum.

No significant differences of MD, RD, or AD were detected in the frontal tracts of the ASD subjects.

3.4. Laterality of the ILF

FA values were more significantly affected in the right ILF than in the left ILF for both the ASD and SPD subjects. While the FA in the left ILF trended lower for both cohorts, only the right side was independently statistically different than that of the TDC subjects. This finding is consistent with a prior finding from Tavor et al. (2013) that face recognition was highly associated with the FA of the ILF in the right hemisphere, and with other previous studies demonstrating right hemisphere dominance in face recognition (Rhodes, 1985; Luh et al., 1991).

3.5 Accounting for performance IQ

Because performance IQ (PIQ) was significantly lower in the ASD cohort compared to the TDC subjects, group differences in FA were also computed while controlling for PIQ scores. After controlling for PIQ, FA for the ASD cohort was still significantly decreased in the fusiform to amygdala, fusiform to hippocampus, and dorsal visual stream at a significance level of $p < 0.05$. The results for the SPD subjects were unchanged.

4. Discussion

This study validates and builds upon previous work demonstrating impaired white matter microstructural integrity in children with SPD and children with ASD, and is the first to compare white matter pathology between these two cohorts. Our method of tractography-based tract delineation allows for the hypothesis-driven

identification of specific white matter tracts that are commonly and differentially affected in SPD and ASD. The results demonstrate differential white matter pathology between SPD and ASD, with temporal tracts traditionally associated with ASD being unaffected in SPD, and with SPD subjects demonstrating more severe white matter pathology in primary sensory processing tracts.

The SPD subjects were most affected in the parieto-occipital tracts, demonstrating trends towards decreased FA and elevated MD and RD in every tract. While both cohorts were affected in these primary sensory processing tracts, the SPD subjects were pervasively more affected, which may reflect the fact that sensory processing difficulties were what brought the children with SPD to medical attention whereas sensory processing issues are typically not the paramount clinical feature in ASD.

In contrast, temporal connectivity seemed to be mainly affected in the ASD subjects, consistent with previous work with white matter pathology in ASD (Travers et al, 2012). The preservation of microstructural integrity in these tracts of the SPD cohort suggests independence of these tracts from the sensory processing differences of children with SPD, and indicates a more direct association between decreased integrity within these tracts and impaired social and emotional processing.

The frontal white matter tracts were not as affected for either SPD or ASD, though the ASD subjects exhibited significantly higher FA in the ACR than the TDC subjects. Though the cellular mechanisms underlying pathologic increase in FA are not well-understood, several factors could be contributors, including increases

in myelination, greater collimation of axonal fibers, and/or increases in axonal diameter and packing density (Beaulieu, 2002). Prior studies have shown increased FA as a reflection of compensatory mechanisms (Holzapfel et al., 2006), and elevated FA is commonly reported in studies of ASD, though the majority of these have included younger subjects (Travers et al., 2012).

Homologous white matter tracts were combined in the results shown here for the purposes of the consolidation of results, and for statistical power. However, group differences were initially computed unilaterally for each tract. In all cases, the results shown here agree with trends or statistically significant group difference results from the component unilateral tracts.

The amount of tract overlap was presented in the results to evaluate the independence of our group difference results. A significant portion of the fusiform to amygdala tract is contained within the fusiform to hippocampus tract, along with the ILF contained within the dorsal visual stream, and the PTR contained within the PCR. Despite these overlaps, however, the group difference results differ between overlapping tracts and provide independently valuable information about functional connectivity in these subjects.

This investigation of white matter microstructure in SPD and ASD subjects is limited by its small sample size, and should be replicated using larger cohorts. Furthermore, while all of the subjects were boys aged 8-11 to increase homogeneity of the study groups, the IQ of the ASD cohort was significantly lower than that of the SPD and TDC cohorts. Further research is therefore needed

to determine whether these findings generalize to other ages, genders, and intellectual abilities.

Future research will include investigation of functional connectivity using resting state fMRI data and magnetic encephalography (MEG) data, which have been previously acquired for these cohorts (unpublished data). The ROIs used to determine structural connectivity in this study could be used to assess differences in functional connectivity between these same regions, with hypothesized decreased functional coupling where decreased structural connectivity was found. While prior studies have found relations between functional connectivity and white matter volume in ASD, there have been no reported relations between functional connectivity and DTI measures in ASD or SPD.

It would also be valuable to investigate the use of more sophisticated models for diffusion such as neurite orientation dispersion and density imaging (NODDI), a new diffusion MRI technique used to estimate microstructural complexity of dendrites and axons with more specific markers of tissue microstructure than the conventional diffusion parameters. However, more sophisticated modeling such as NODDI requires a more intensive diffusion imaging protocol with longer data acquisition at multiple b values (a parameter defined by gradient strength and RF pulse separation that determines the amount of diffusion weighting) (Zhang et al., 2012).

5. Conclusion

While sensory processing differences are known to be associated with other neuropathologies such as autism, SPD in isolation is poorly understood. This study validates and expands upon preliminary studies of white matter pathology in SPD, and provides evidence that SPD is a disorder in which the white matter microstructure provides differential characterization from the sensory processing differences that manifest in ASD.

References

- R.R. Ahn, L.J. Miller, S. Milberger, D.N. McIntosh. Prevalence of parents' perceptions of sensory processing disorders among kindergarten children. *American Journal of Occupational Therapy*, 58 (2004), pp. 287–293.
- American Psychiatric Association Diagnostic and statistical manual of mental disorders: DSM-IV. 4th Ed. American Psychiatric Association; Washington, D.C.: 1994.
- Baranek, G. T., Boyd, B. A., Poe, M. D., David, F. J., and Watson, L. R. (2007). Hyperresponsive sensory patterns in young children with autism, developmental delay, and typical development. *Am. J. Ment. Retard.* 112, 233–245.
- P.J. Basser, J. Mattiello, D. LeBihan. MR diffusion tensor spectroscopy and imaging. *Biophysical Journal*, 66 (1994), pp. 259–267.
- Beaulieu C (2002) The basis of anisotropic water diffusion in the nervous system—a technical review. *NMR Biomed* 15:435–455.
- A. Ben-Sasson, L. Hen, R. Fluss, S.A. Cermak, B. Engel-Yeger, E. Gal. A meta-analysis of sensory modulation symptoms in individuals with autism spectrum disorders. *Journal of Autism and Developmental Disorders*, 39 (2009), pp. 1–11.
- B.A. Brett-Green, L.J. Miller, W.J. Gavin, P.L. Davies. Multisensory integration in children: a preliminary ERP study. *Brain Research*, 1242 (2008), pp. 283–290.
- A.C. Bundy, S. Shia, L. Qi, L.J. Miller. How does sensory processing dysfunction affect play? *American Journal of Occupational Therapy*, 61 (2007), pp. 201–208.
- W. Dunn, K. Westman. The sensory profile: the performance of a national sample of children without disabilities. *American Journal of Occupational Therapy*, 51 (1997), pp. 25–34.
- L.C. Eaves, H.D. Wingert, H.H. Ho, E.C. Mickelson. Screening for autism spectrum disorders with the social communication questionnaire. *Journal of Developmental and Behavioral Pediatrics*, 27 (Suppl. 2) (2006), pp. S95–S103.
- B. Fischl. FreeSurfer. *NeuroImage*, 62 (2012), pp. 774–781.
- Holzappel M, Barnea-Goraly N, Eckert MA, Kesler SR, Reiss AL (2006) Selective alterations of white matter associated with visuospatial and sensorimotor dysfunction in Turner syndrome. *J Neurosci* 26:7007–7013.
- M. Jenkinson, P. Bannister, M. Brady, S. Smith. Improved optimization for the robust and accurate linear registration and motion correction of brain images. *NeuroImage*, 17 (2002), pp. 825–841.
- C. Lord, M. Rutter, S. Goode *et al.* Autism diagnostic observation schedule: a standardized observation of communicative and social behavior. *Journal of Autism and Developmental Disorders*, 19 (1989), pp. 185–212.

C. Lord, M. Rutter, A. Le Couteur. Autism diagnostic interview-revised: a revised version of a diagnostic interview for caregivers of individuals with possible pervasive developmental disorders. *Journal of Autism and Developmental Disorders*, 24 (1994), pp. 659–685.

Luh, K.E., Rueckert, L.M., Levy, J., 1991. Perceptual asymmetries for free viewing of several types of chimeric stimuli. *Brain Cogn* 16, 83–103.

Marco EJ, Hinkley LB, Hill SS, Nagarajan SS. Sensory processing in autism: a review of neurophysiologic findings. *Pediatr Res*. 2011;69(5 Pt 2):48R–54R.

S. Mori, B.J. Crain, V.P. Chacko, P.C. van Zijl. Three-dimensional tracking of axonal projections in the brain by magnetic resonance imaging. *Annals of Neurology*, 45 (1999), pp. 265–269.

P. Mukherjee, J.I. Berman, S.W. Chung, C.P. Hess, R.G. Henry. Diffusion tensor MR imaging and fiber tractography: theoretic underpinnings. *AJNR. American Journal of Neuroradiology*, 29 (2008), pp. 632–641.

Nichols T, Holmes A (2001) Nonparametric permutation tests for functional neuroimaging: a primer with examples. *Human Brain Mapping* 15: 1–25.

Julia P. Owen, Elysa J. Marco, Shivani Desai, Emily Fourie, Julia Harris, Susanna S. Hill, Anne B. Arnett, Pratik Mukherjee. Abnormal white matter microstructure in children with sensory processing disorders. *NeuroImage: Clinical*, Volume 2, 2013, Pages 844–853.

Rhodes, G., 1985. Lateralized processes in face recognition. *Br J Psychol* 76 (Pt 2), 249–71.

S.A. Schoen, L.J. Miller, B.A. Brett-Green, D.M. Nielsen. Physiological and behavioral differences in sensory processing: a comparison of children with autism disorder and sensory modulation disorder. *Front Integr Neurosci*, 3 (2009), p. 29 Epub.

Tavor, Ido, Yablonski, Maya, Mezer, Aviv, Rom, Shirley, Assaf, Yaniv, Yovel, Galit, Separate parts of occipito-temporal white matter fibers are associated with recognition of faces and places, *NeuroImage* (2013), doi: 10.1016/j.neuroimage.2013.07.085

B.G. Travers, N. Adluru, C. Ennis *et al.* Diffusion tensor imaging in autism spectrum disorder: a review. *Autism Research*, 5 (2012), pp. 289–313

D. Wechsler. WISC-IV: Administration and Scoring Manual. Psychological Corporation (2003).

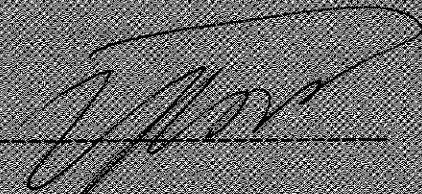
Zhang H., Schnneider T., Wheeler-Kingshott C. A., Alexander D. C. (2012). NODDI: practical *in vivo* neurite orientation dispersion and density imaging of the human brain. *Neuroimage* 61, 1000–1016. doi: 10.1016/j.neuroimage.2012.03.072.

Publishing Agreement

It is the policy of the University to encourage the distribution of all theses, dissertations, and manuscripts copies of all UCSF theses, dissertations, and manuscripts will be routed to the library via the Graduate Division. The library will make all theses, dissertations, and manuscripts accessible to the public and will preserve these to the best of their ability, in perpetuity.

Please sign the following statement:

I hereby grant permission to the Graduate Division of the University of California, San Francisco to release copies of my thesis, dissertation, or manuscript to the Campus Library to provide access and preservation, in whole or in part, in perpetuity.



Author Signature

9/10/13
Date